The lattice site of Ti in $LiNbO_3$

1994 J. Phys.: Condens. Matter 6 267

(http://iopscience.iop.org/0953-8984/6/1/026)

J. Phys.: Condens. Matter 6 (1994) 267–274. Printed in the UK

The lattice site of Ti in $LiNbO_3$

B Hauer†¶, R Vianden†, M F da Silva‡, L Rebouta§††, J C Soares§, E Dieguez‖ and F Agullo-Lopez‖

† Institut für Strahlen- und Kernphysik, Universität Bonn, Bonn, Federal Republic of Germany
‡ Departamento de Fisica, ICEN, LNETI, Sacavem, Portugal
§ CFNUL da Universidade de Lisboa, Lisbon, Portugal
‖ Departamento de Fisica de Materiales C-IV, Universidade Autonoma de Madrid, Madrid, Spain

Received 6 May 1993, in final form 31 August 1993

Abstract. The site of Ti in $LiNbO_3$ was studied by means of γ–γ perturbed angular correlation and the PIXE–channelling technique. It is found that, after in-diffusion, Ti is situated in the oxygen octahedron normally occupied by a Li ion. However, evidence for association with a defect or slight displacement from the ideal site is observed.

1. Introduction

$LiNbO_3$ is a material [1] with important applications for bulk and waveguide optoelectronic devices owing to its high electro-optic coefficients, its transparency range and the availability of large and good-quality single crystals. Further a large number of potential applications for information storage and real-time holography relies on its photorefractive behaviour [2].

It is known that the photorefractive effect is strongly influenced by the presence of transition-metal impurities [3]. However, until recently, no definite information about the site of the transition metals (e.g. Fe) in the $LiNbO_3$ lattice was available. Then it was shown by Rebouta *et al* [4] that, in contrast with the widespread assumption that Fe occupies the Nb site in $LiNbO_3$, it occupies the Li site instead. In view of these results and the importance of the lattice site of dopants for the theoretical understanding and any predictions about the location of energy levels as well as electron- or hole-trapping capabilities, in the present study the lattice surrounding and the site of the technically important Ti impurity were investigated.

To this end a nuclear technique, namely the γ–γ perturbed angular correlation (PAC) technique [5] was applied, since it is extremely sensitive to lattice disorder in the nearest-neighbourhood of the atom under investigation and since a suitable probe atom ^{44}Ti is available. On the other hand, the PIXE–channelling technique provides information about the location of the Ti ion relative to the distant undisturbed lattice and thus allows identification of the lattice site occupied by the Ti ion.

¶ Present address: IFF Kernforschungsanlage Jülich, W-5170 Jülich, Federal Republic of Germany.
†† Present address: Departamento de Fisica, Universidade do Minho, Azurem, P-4800 Guimaraes, Portugal.

0953-8984/94/010267+08$07.50

2. Experimental details

Congruent $LiNbO_3$ crystals were grown under an oxygen atmosphere by the Czochralski method from grade I Johnson–Matthey powder. Plates were cut both perpendicular and parallel to the $\hat{c}$ axis, polished with 0.3 μm alumina powder and used without further treatment for the PAC experiments. For the RBS–PIXE experiments the $LiNbO_3$ crystals were doped during growth by adding 1% TiO_2 to the melt.

The γ–γ PAC technique probes the interaction between the nuclear quadrupole moment of a suitable nucleus and the electric field gradients (EFGs) produced by surrounding electric charges, e.g. by ions in a crystal lattice. Because of its symmetry properties the EFG tensor vanishes if the charge symmetry about a particular lattice site is of cubic or higher symmetry. Owing to the $1/r^3$ dependence of the magnitude of the EFG, only deviations from perfect symmetry in the first- or second-nearest-neighbour shell lead to large effects and thus make the PAC technique an ideal tool for the study of the microscopic lattice surrounding of impurities (dopants) at extremely low concentrations.

The PAC probe has to be an unstable nucleus, which during its decay populates a γ–γ cascade of a daughter nucleus. In the present case the isotope ^{44}Ti decays to ^{44}Sc (figure 1). Because of the conservation of the angular momentum the emission directions of the γ-rays populating and depopulating the intermediate nuclear state are correlated. This correlation is changed by quadrupolar interaction between the quadrupole moment of the nucleus in the intermediate state and an EFG and leads in a semiclassical picture to precession of the nuclear spin about the symmetry axis of the EFG. This in turn causes a modulation of the angular correlation pattern depending on the time spent in the intermediate state. Details of the application of the PAC technique to the study of defects in materials can be found in the literature [6].

The parent radioactivity for the present study, ^{44}Ti ($t_{1/2}$ = 49 years [7]), was obtained commercially [8]. Ideally identical sample preparation procedures for the RBS–PIXE and PAC measurements would have been desirable. However, the growth of ^{44}Ti doped crystals from the melt would have required a large amount of radioactivity which, owing to the long half-life of ^{44}Ti, would have led to intolerable contamination of the growth equipment. Therefore the radioactivity had to be diffused into the $LiNbO_3$ crystals. To this end, approximately 4 kBq of ^{44}Ti dissolved in 0.1 N HCl was dried on 4 mm × 2 mm × 0.7 mm $LiNbO_3$ crystals with the surface plane parallel to the $\hat{c}$ axis. The Ti in-diffusion was carried out in a quartz tube where the sample was heated in air first for 18 h to 1200 K and next in a second step for 22 h to 1320 K; it was then slowly cooled to room temperature. No special measures were taken to prevent Li out-diffusion. The known diffusion constant for Ti in $LiNbO_3$ of $D = 1.1 \times 10^{-12}$ cm^2 s^{-1} [1] at 1320 K allows us to estimate a mean square penetration depth of $(6\ \mu\text{m})^2$ with a maximum concentration of the Ti ions close to the surface of 2×10^{17} cm^{-3}.

The 78–68 keV γ–γ cascade in ^{44}Sc (figure 1) was used for the PAC measurements. The intermediate state has a half-life $t_{1/2}$ = 153 ns and a spin $I = 1$; its quadrupole moment has been determined to be $Q = 0.21(2)$b [9]. The anisotropy coefficient of the cascade has a value of $A_{22} = 0.045(3)$ [10].

A four-detector set-up equipped with BaF_2 scintillators was used for the PAC measurements. They were arranged in a plane forming angles of 90° between adjacent detectors. The shape of the scintillators (cut cones) and the distance of only 10 mm to the sample ensured a large solid angle which allowed us to work with very weak sources. Owing to the low energies of the 78–68 keV γ–γ cascade, specially developed constant-fraction discriminators were used to obtain a good response and time resolution [11].

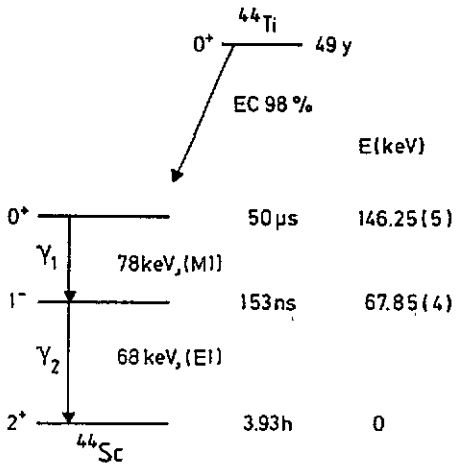

Figure 1. Partial decay scheme of ^{44}Ti with the γ–γ cascade used for the experiments.

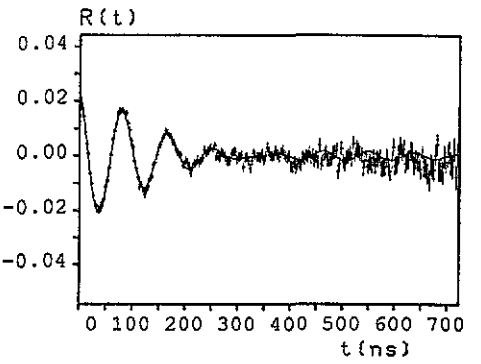

Figure 2. Time-dependent anisotropy for the 78–68 keV γ–γ cascade of ^{44}Sc in a $LiNbO_3$ single crystal with its $\hat{c}$ axis aligned with the angle bisector of two adjacent detectors. (The constant C due to the angle-dependent absorption has been subtracted from the data.)

Delayed coincidence spectra $N(\theta, t)$ were recorded automatically for interdetector angles of $\theta = 90°$ and 180°. From these the time differential anisotropy $R(t) = 2[N(180°, t) - N(90°, t)]/[N(180°, t) + 2N(90°, t)]$ was computed. The result for an orientation of the $\hat{c}$ axis of the crystal parallel to the angle bisector of two adjacent detectors is shown in figure 2. In figures 3(a) and 3(b) spectra taken with the same sample but for an orientation of the $\hat{c}$ axis perpendicular to the plane of the detectors and parallel to the symmetry axis of a 180° detector pair, respectively, are shown.

RBS and PIXE–channelling experiments were performed using a three-axis goniometer at the 4 MV accelerator of the CNRS–Strasbourg Van de Graaff laboratory. A proton beam of 1.5 MeV and typical currents of 5 nA were used in the experiments. For the PIXE analysis a Si(Li) x-ray detector with a resolution of 180 eV placed at an angle of 150° to the beam direction was used. The scattered proton spectra were measured using a silicon surface barrier detector with a resolution of 16 keV at 160° to the beam direction.

Further RBS and NRA–channelling experiments were carried out in the channelling line of the 2 MeV Van de Graaff of LNETI, Sacavem, using 1.6 MeV protons. The back-scattered protons and α-particles from the ^{7}Li(p, α)^{4}He reaction were detected at an angle of 140° and 180° using two silicon surface barrier detectors with resolutions of 13 keV and 18 keV respectively. At 180° the energy of the α-particles produced by the nuclear reaction is 7.529 MeV.

3. Results and discussion

3.1. PAC measurements

Under the assumption that the Ti ion is located on the symmetry axis of the crystal (e.g. in the ideal Nb, Li or octahedral site), one expects the main component of the crystal EFG V_{zz}

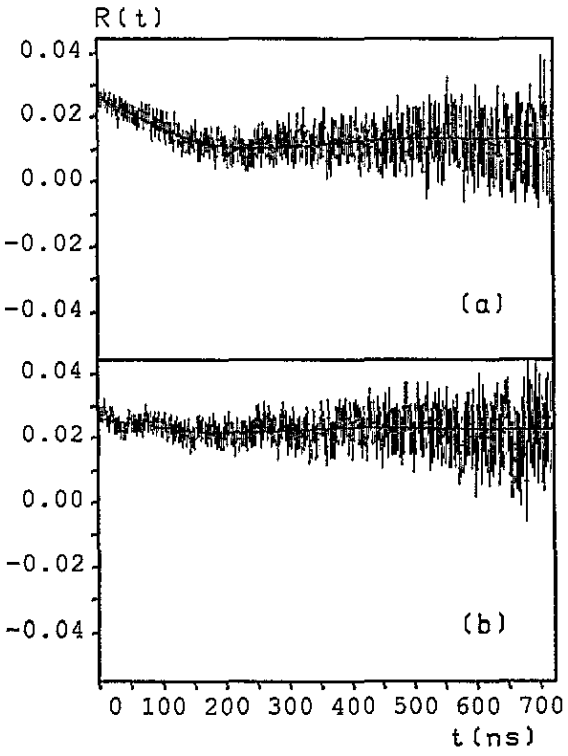

Figure 3. Time-dependent anisotropy for the 78–68 keV γ–γ cascade of ^{44}Sc in a $LiNbO_3$ single crystal with its $\hat{c}$ axis (*a*) perpendicular to the detector plane and (*b*) parallel to the axis of a 180° detector pair. (The constant C due to the angle-dependent absorption has been subtracted from the data.)

to be parallel to the $\hat{c}$ axis and axial symmetry of the EFG, i.e. $\eta = 0$. Generally, for an orientation of the crystal $\hat{c}$ axis parallel to the angle bisector of two neighbouring detectors, the time dependence of the anisotropy $R(t)$ can be described theoretically by the function

$$R(t) = \tfrac{1}{2}A_{22}[\cos(\omega_2 t) + \cos(\omega_3 t)] \tag{1}$$

with $\omega_{2,3} = (3 \mp \eta)\omega_Q$. The so-called quadrupole interaction frequency ω_Q is given by

$$\omega_Q = eV_{zz}Q/[4I(2I-1)\hbar] \tag{2}$$

with e the elementary charge, V_{zz} the principal component of the EFG, I the spin and Q the quadrupole moment of the intermediate state. In the literature usually the spin-independent quadrupole coupling constant

$$\nu_Q = eV_{zz}Q/h \tag{3}$$

is given.

The data in figure 2 show a well defined quadrupole interaction pattern with the full anisotropy expected for the γ–γ cascade of ^{44}Ti after correction for the reduction caused by the finite solid angle of the detectors. This indicates that about 100% of the ^{44}Ti probe atoms occupy the same unique lattice site and that the diffusion step did not lead to destruction of the crystal surface due to Li or O losses. A least-squares computer program adjusted the parameters of equation (1) to fit the spectrum with the value of η kept fixed to 0, i.e. $\omega_2 = \omega_3$. To allow for a slight distribution of EFGs a frequency distribution of Lorentzian

shape was taken into account by a multiplicative factor $\exp(-\delta\omega t)$. Further, since the radioactive ^{44}Ti was diffused into the crystal from only one side, some γ-rays had to travel through the crystal whereas others did not have to. Because of the relatively low γ energies of the ^{44}Ti cascade this led to an angle-dependent absorption which causes a constant shift in the $R(t)$-values. To correct for this effect a constant C was added to the fitted function in equation (1).

The results of the fit are $A_{22} = 0.026(1)$, $\nu_Q = 15.3(2)$ MHz and $C = -0.0190(2)$. The frequency distribution parameter δ had a value of 0.088(3). This is in perfect agreement with the assumption made above about the orientation and symmetry of the EFG at the Ti site. However, before discussing the results (especially the origin of the damping of the precession pattern), one has to consider also the possibility that the asymmetry parameter η is not equal to 0. In the present case for the spin $I = 1$ of the intermediate level a value of $\eta > 0$ lifts the degeneracy of the $m = \pm 1$ level, leading to the appearance of two very similar frequencies ω_2 and ω_3. In the range $0 < \eta < 0.25$ this causes a beat pattern in the precession which in the time range set by the half-life of the intermediate state is indistinguishable from damping caused for instance by imperfections in the crystal lattice surrounding the Ti probes. The best fit to the data is obtained for a value of η fixed to 0.19 with δ being reduced to 0.059(3) (full curve in figure 2). Owing to the weak influence of η through $\omega_{2,3}$ on the quadrupole interaction frequency, ν_Q remains almost unchanged at 15.4(2) MHz.

Measurements under different orientations of the crystal relative to the detectors could resolve this ambiguity. For an orientation of the $\hat{c}$ axis perpendicular to the detector plane, one would expect the following perturbation function:

$$R(t) = \tfrac{1}{2}A_{22}[1 + \cos(\omega_1 t)] \qquad \text{with } \omega_1 = 2\eta\omega_Q \tag{4}$$

i.e. $R(t) =$ constant for $\eta = 0$. The data taken in this orientation (figure 3(*a*)) show primarily the absence of any fast modulation which is in agreement with the above interpretation. However, the $R(t)$-values are not constant as expected from equation (4) for $\eta = 0$. Instead they show a slow modulation which cannot be described by the above expression unless again a multiplicative factor $\exp(-\delta\omega t)$ allowing for a frequency distribution is included. Then a fit of equation (4) to the data yields values of ω_1 between 7 and 13 Mrad s^{-1}. The large uncertainty is due to the strong correlation with the damping constant δ which assumes values between 1.0 and 0.45, respectively. The additive constant C remains unchanged at -0.019 as expected since the change in crystal orientation involves a rotation only about the face normal, thus leaving the angle-dependent γ absorption unchanged.

Using the relation $\eta = \omega_1/2\omega_Q$, one obtains $0.14 \leqslant \eta \leqslant 0.27$ in agreement with $\eta = 0.19$ derived above. A more precise determination of the frequency and thus η is impossible because of the strong damping which is considerably larger (up to ten times) than in the previous measurement.

A consistent result is obtained from the measurement with the $\hat{c}$ axis aligned with a pair of detectors. On the basis of the above model, again no fast modulation is expected theoretically. The data are indeed quite time independent (figure 3(*b*)) but also here they can be described better if a small quadrupole interaction frequency with a large damping is included in the fit.

The problem of the substantially different damping observed for the different orientations of the crystal can be understood if one considers in detail the influence of a distribution of EFGs around a mean value on the distribution of the three quadrupole interaction frequencies ω_{1-3} and the damping factors δ_{1-3}. A detailed calculation [12], assuming Gaussian

distributions of the components of the EFG tensor, shows that in the case where $I = 1$, δ_1 becomes proportional to $1/\eta$ whereas δ_2 and δ_3 are proportional to $1/(3 \mp \eta)$. This in general causes different damping factors for the quadrupole interaction frequencies observed in different orientations and, for small values of η especially, it leads to a large increase of δ_1 as compared to $\delta_{2,3}$, which are similar in this case. So, for example, for $\eta = 0.2$ and a relative width $\Delta\eta = 0.1$ a factor of $\simeq 5$ is estimated for the ratio $\delta_1/\delta_{2,3}$. This explains at least qualitatively the differences in δ observed for the different crystal orientations, since it can be expected that a similar effect would be found if Lorentzian instead of Gaussian distributions for the EFGs are employed.

Summarizing, one can conclude that the PAC results show the presence of a largely unique EFG at the site of the ^{44}Ti probes in $LiNbO_3$ and are also consistent with the assumption that the main component V_{zz} of the EFG is oriented parallel to the $\hat{c}$ axis of the crystal lattice. From the measured quadrupole interaction frequency $\nu_Q = 15.4(2)$ MHz an EFG of $V_{zz} = 3.0(3) \times 10^{17}$ V cm^2 can be derived.

However, the data strongly indicate that the asymmetry parameter η is not equal to 0 as expected. Its value cannot be determined precisely but can be restricted to the interval $0.14 \leqslant \eta \leqslant 0.25$ with the best fit obtained for $\eta = 0.19$. This could be explained by a small displacement of the Ti probes from the ideal Li lattice site. A more probable cause, however, is the association of the Ti impurity with an intrinsic defect of the $LiNbO_3$ lattice. In congruent $LiNbO_3$ the most numerous intrinsic defects are vacancies in the Nb sublattice and the so-called antisite defects Nb_{Li}, i.e. Nb atoms occupying Li sites [12]. The presence of such defects in an off-axis position near the Ti probe could be responsible for the experimentally observed asymmetry of the EFG.

3.2. PIXE–channelling results

In the PIXE measurements the Ti Kα x-rays were collected as the Ti signal, and the Nb L x-rays as the Nb signal. In figure 4 the angular scans taken with the Ti-doped $LiNbO_3$ sample through $\langle 0001 \rangle$, $\langle 02\bar{2}1 \rangle$ and $\langle 04\bar{4}1 \rangle$ axial and (0001) planar directions are presented.

In the $\langle 0001 \rangle$ angular scan, the Nb and Ti dips show a similar behaviour, indicating that the Ti ions are perfectly substitutional with regard to the Nb rows which constitute the $\langle 0001 \rangle$ channel. Therefore an occupation of the tetrahedral sites by the Ti ions (figure 5) can be excluded. However, it leaves the possibility that the Ti ions occupy the Li sites and/or the free octahedral sites because those sites are shadowed by Nb atoms along this direction. From the Ti and Nb dips in the $\langle 04\bar{4}1 \rangle$ angular scan, we can further exclude the occupation of a position in the vicinity of the free octahedral site.

In the results for the $\langle 02\bar{2}1 \rangle$ and $\langle 11\bar{2}0 \rangle$ axes, displayed in figure 4, the Ti dips are narrower than the respective Nb dips. These results are not compatible with the assumption that the Ti ions are dissolved on Nb sites, which leaves as the most probable possibility occupation of the Li site. This conclusion is also supported by the flux peak observed in the (0001) planar direction.

In order to make possible a qualitative comparison between the PIXE data and the angular scans obtained with particles also the yield of the α-particles induced by the ^{7}Li(p, α)^{4}He reaction as well as the yield of back-scattered protons as functions of the angle for the $\langle 02\bar{2}1 \rangle$ axial and (0001) planar directions were measured.

For the comparison we assumed that the x-ray production in one layer parallel to the surface when the proton beam is aligned with a crystallographic direction is approximately proportional to the flux of the back-scattered protons, i.e. that it is proportional to the RBS yield corresponding to that layer. Although the PIXE spectra have no depth resolution, we can calculate the contribution of each layer to the collected x-rays. Thus, the angular scans

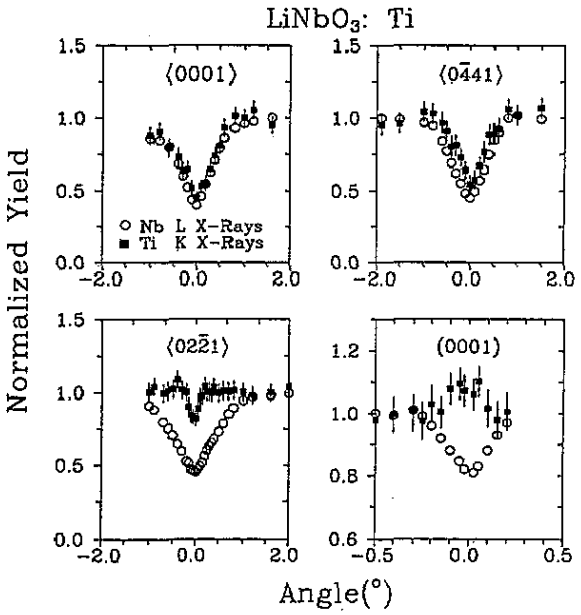

Figure 4. Angular dependence of the normalized Nb L x-ray emission yield (○) and the Ti Kα x-ray emission yield (■) obtained in scans through axial and planar directions as indicated for a congruent $LiNbO_3$ sample doped with 1% Ti.

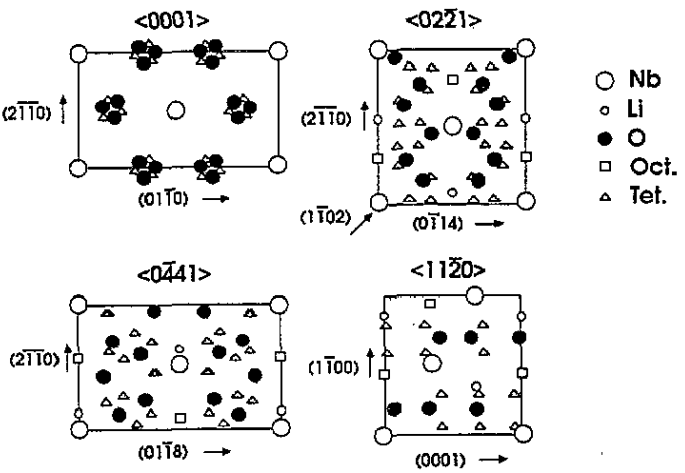

Figure 5. Projection of regular lattice sites of $LiNbO_3$ onto planes perpendicular to directions used in axial channelling experiments: ○, Nb sites; ○, Li sites; ●, O sites; □, free octahedral sites; △, tetragonal sites.

presented in figure 6 were obtained by weighting the contribution of layers of about 0.25 μm up to a depth of about 3 μm from the back-scattered particle spectra, taking into account the production of x-rays in each layer and the respective absorptions. We can then compare the angular scans shown in figures 4 and 6. The similarity between these angular scans

supports the conclusion obtained above, that Ti ions occupy predominantly the Li site, a result which is also in good agreement with PIXE–channelling measurements reported by Kollewe *et al* [13] for comparably low Ti concentrations.

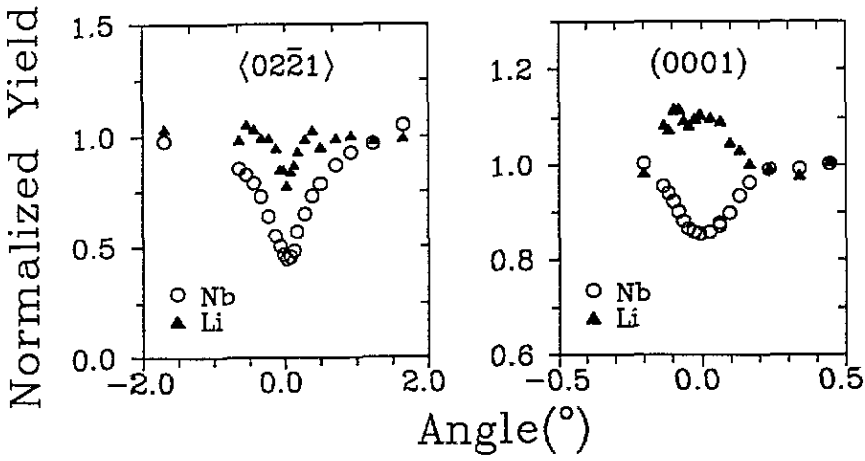

Figure 6. Angular dependence of the normalized back-scattering yield of 1.6 MeV H^+ ions from Nb (○) and α-particles of the $^7Li(p, \alpha)^4He$ reaction (▲).

Acknowledgments

This work has been supported in part by the Bundesminister für Forschung und Technologie under grant 03-BO1BON-2, the EC under contract SC 1.0049.C(H) and NATO under grant CRG 890934. One of us (LR) thanks the Junta Nacional de Investigacao Cientifica e Tecnologica for a fellowship under the Science Program.

References

[1] *Properties of $LiNbO_3$ (EMIS Datareviews Series 5)* 1989 (London: INSPEC)
[2] Günter P and Huignard J P (ed) 1988 *Photorefractive Materials and their Applications* vol I (Berlin: Springer); 1989 *Photorefractive Materials and their Applications* vol II (Berlin: Springer)
[3] See, e.g.,
Alferness R C 1986 *Science* **234** 825
[4] Rebouta L, DaSilva M F, Soares J C, Hage-Ali M, Stoquert J P, Siffert P, Sanz-Garcia J A, Dieguez E and Agullo-Lopez F 1991 *Europhys. Lett.* **14** 557
[5] Steffen R M and Alder K 1975 *The Electromagnetic Interaction in Nuclear Spectroscopy* ed W D Hamilton (Amsterdam: North-Holland)
[6] Vianden R 1988 *Nato ASI Series E* vol 144, p 239
[7] Endt P M 1990 *Nucl. Phys.* A **521** 1
[8] Obtained from Medgenix GmbH, Düsseldorf, Federal Republic of Germany.
[9] Haas H and Shirley D A 1973 *J. Chem. Phys.* **58** 3339
[10] Glass J C and Kliwer J K 1968 *Nucl. Phys.* A **115** 234
[11] Schaefer Th 1992 *Thesis* University of Bonn
[12] Schirmer O F, Thiemann O and Wöhlecke M 1991 *J. Phys. Chem. Solids* **52** 185
[13] Kollewe D, Kling A, Grabmeier B C, Bremer T, Heiland W and Zimmermann W 1992 *Phys. Lett.* **169A** 177